　http://www.journalmt.com

Possibilities for Improvement of Mechanical Properties of High-Strength Medium-Carbon SiCr Steels

Pavel Salvetr (0000-0001-5717-267X)[1], Jakub Kotous (0000-0001-9141-8477)[1], Črtomir Donik (0000-0001-6531-8771)[2], Aleksandr Gokhman (0000-0002-0533-2114)[1], Zbyšek Nový (0000-0001-6976-1578)[1]
[1]COMTES FHT a.s., Průmyslová 995, 334 41 Dobřany. Czech Republic. E-mail: Pavel.Salvetr@comtesfht.cz
[2]Institute of Metals and Technology (IMT), Lepi pot 11, 1000 Ljubljana. Slovenia. E-mail: Crtomir.Donik@imt.si

The 54SiCr6 high-strength low-alloyed steel with medium carbon content is studied in this work. Its excellent mechanical properties allow a wide range of applications as springs and vibration dampers. The high strength is usually achieved during heat treatment consisting of quenching and tempering. This manuscript represents several methods to further increase in mechanical properties. Firstly, the influence of Accelerated Carbide Spheroidization and Refinement (ASR) on microstructure before quenching and tempering was studied and enhanced plastic properties were measured. Secondly, a thermomechanical treatment before quenching increased the strength. Finally, the use of strain assisted tempering caused a further strengthening effect compared to conventional tempering. All these methods improve mechanical properties, some increase strength and others ductility.

Keywords: Spring steel, 54SiCr6 steel, Microstructure, Mechanical properties

1 Introduction

54SiCr6 (1.7102) is a low alloyed steel containing medium carbon content and alloyed with chromium and silicon. Good mechanical properties, such as high strength, fracture toughness, ductility and fatigue resistance make this steel attractive for use as high-stressed automotive suspension springs, bumper rings of railways wagons and other dumpers or structural parts. The required mechanical properties are usually achieved by quenching and tempering which provide near-fully martensitic microstructure. The following conditions of heat treatment are given for the 54SiCr6 steel in ISO 8458-1 standard: quenching temperature in the range of 840 °C and 870 °C, quenching medium – oil and tempering temperature between 400 °C and 450 °C. These conditions result in yield strength ($R_{p0.2}$) of 1300 MPa at least, ultimate tensile strength (R_m) 1450 – 1750 MPa, 6 % of elongation (A_5) at least, reduction of area (Z) of 25 % and impact energy for 20 °C of 8 J at least [1].

Quenching of carbon steels provides a formation of a martensite structure in order to increase the yield strength. Thus, the as-quenched state appears to have a high yield strength but limited plastic properties. At the same time, the microstructure consists of martensite and retained austenite, and a dislocation density is very high [2–4]. Residual stress release and several microstructural transformations occur during tempering. In tempering stage „0", carbon atoms segregation and cluster formation occur on dislocations and lath boundary up to the temperature of 100 °C. The transition carbides (η-Fe_2C and ε-Fe2.4C)

precipitate during the tempering stage „1" and a volume decreases (80 – 200 °C). On the contrary, the volume increases during the further tempering stage „2" due to retained austenite decomposition into ferrite and cementite in the temperature range of 200 – 300 °C. In the tempering stage „3", segregated carbon and transition carbides transform to cementite between 250 °C and 480 °C and a volume of dilatometric specimen decreases in this stage. Tempering at higher tempering temperatures causes spheroidization and coarsening of cementite, recovery and recrystallization of ferrite [5–7]. The decomposition of austenite into ferrite and cementite can result in a sharp decrease in impact toughness due to of tempering martensite embrittlement (TME) [8–12]. The above-mentioned temperature ranges for individual stages of tempering may vary depending on the chemical composition. Previous studies [8, 13] reported the effect of silicon on the temperatures of microstructural changes during tempering. Silicon retards and delays the formation of transition carbides, retained austenite decomposition and cementite formation and shifts the temperature range for TME to higher tempering temperatures as well [8, 12, 13]. Furthermore, silicon significantly strengthens a ferrite/martensite matrix via solid solution strengthening. The degree of solid solution strengthening by silicon is about 83 MPa per 1 wt.% of Si solute in a matrix [14, 15].

In this work, possibilities for further improvement of the mechanical properties of the 54SiCr6 steel were investigated in comparison with conventional heat

treatment. The refinement of carbides using Accelerated Carbide Spheroidization and Refinement (ASR) before hardening was examined. ASR processing provides a very fine microstructure before quenching and tempering. Thermomechanical treatment (TMT) of steel before quenching was also examined. This treatment utilizes plastic deformation of austenite before quenching resulting in a fine microstructure with high strength. A further approach called strain-assisted tempering (SAT) aimed to improve mechanical properties during tempering. SAT treatments consist of first tempering, cooling, deformation, second tempering and final cooling.

2 Experimental

2.1 Materials and heat treatment

Investigated steel was melted in a vacuum induction furnace and casted into a 45 kg ingot. The chemical composition of steels was determined using Q4 Tasman optical emission spectrometer. The chemical composition of Steel 1 corresponds to the 54SiCr6 steel (1.7102) according to the standard ISO 8458-1:2002. The chemical composition of the studied steel is given in Tab. 1. The ingots were heated up above 1050 °C, forged to blocks, hot-rolled to 14 mm thick plates and air-cooled. Normalisation annealing was performed at 850 °C for 40 min.

Tab. 1 *Chemical compositions of experimental materials in wt. %*

Material	C	Si	Cu	Mn	Cr	Fe
Steel 1	0.57	1.51	0.12	0.68	0.75	Bal.
54SiCr6	0.51-0.59	1.2-1.6	-	0.5-0.8	0.5-0.8	96.2-97.3

2.2 Influence of initial microstructure

To determine the effect of the initial microstructure, the as-normalized and ASR-processed microstructure of the Steel 1 were chosen. The normalisation annealing was carried out at 850 °C for 40 min with subsequent air-cooling. The ASR process includes thermal cycling around the temperature of A_1, overheating above A_1 and undercooling below A_1. In this treatment, three thermal cycles were applied. The first and second thermal cycles are the same – induction heating to 820 °C with the heating rate of 19 °C/s, the soak at 820 °C for 15 s, free cooling to 725 °C and the soak at this temperature for 300 s. In the last round of ASR, the soak at 725 °C is extended to 600 s followed by air cooling. In this state is possible to compare the influence of as-normalized and ASR-processed microstructure on the mechanical properties of steel after quenching from 890 °C (20 min) and tempering at 400 °C for 2 h.

2.3 Influence of thermomechanical processing

The effect of austenite deformation before quenching on the resultant mechanical properties of hardened Steel 1 was studied. The initial microstructure after normalization was chosen. Conventional quenching and tempering (QT) consisted of austenitization at 900 °C for 20 min, followed by oil quenching and tempering at 250 °C for 2 h was applied. Conditions of thermomechanical processing (TMP) were the following – austenitization at 900 °C for 30 min, then follows deformation and oil quenching. No delay included between deformation and quenching – only necessary handling time. The same tempering at 250 °C for 2 hours was performed after quenching. The deformation was proposed by close-die forging. The close-die tool was a split hole 12 mm in diameter. The initial rods were 10 x 16 x 250 mm in dimensions.

A numerical simulation predicted that the deformation was done at the temperature of approx. 830 °C.

2.4 Influence SAT processing

To compare the properties of conventional tempered material and quenched with the following SAT, Steel 1 was austenitized at 900 °C for 20 min, followed by oil quenching. The tempering was carried at 300 °C for 2 h. The SAT treatment included first tempering at 250 °C for 2 h, rotary swagging with a reduction in diameter of about 17%, followed by a second tempering at 300 °C for 2 h and air cooling.

2.5 Microstructure and mechanical properties characterization

Specimens for microstructural investigation were prepared on cut parallel to the longitudinal direction. They were polished using an automatic, microprocessor-controlled machine for grinding and polishing with a final step of polishing performed using OP-S Non-Dry colloidal silica suspension with a particle size of 0.05 μm. The microstructure was revealed by etching in Nital reagent (98 mL of ethanol + 2 mL nitric acid) and observed in the scanning electron microscope JEOl IT 500 HR. X-ray diffraction (XRD) analysis was performed on polished surfaces of samples on a Bruker Advance D8 diffractometer with a cooper anode
(λ Kα1 = 0.15406 nm). The content of retained austenite (RA) was determined in the 2θ range from 30° to 105° with a step size of 0.025°. The electron backscattered diffraction (EBSD) analyses were performed on the polished surface under the following conditions: 20 kV, on the area of 40 x 40 μm and step size of 0.05 μm, tilted for 70°. EBSD analyses were focused on the determinatiom of grain size and misorientation angle distribution.

Mechanical properties were characterized by hardness and tensile tests at ambient temperature. Round tensile samples of 50 mm in gauge length and 8 mm in diameter were tested at a rate of 0.75 mm/min on a Zwick Z250 testing machine (ZwickRoell GmbH & Co. KG, Ulm, Germany) with a 250 kN capacity according to ČSN EN ISO 6892-1. Tensile characteristics were evaluated (e.g., ultimate tensile strength—Rm; yield strength—Rp0.2; Young modulus—E; uniform plastic elongation - Ag; total plastic elongation after a fracture - A5; and reduction in area - Z).

3 Results and discussion

3.1 Influence of initial microstructure
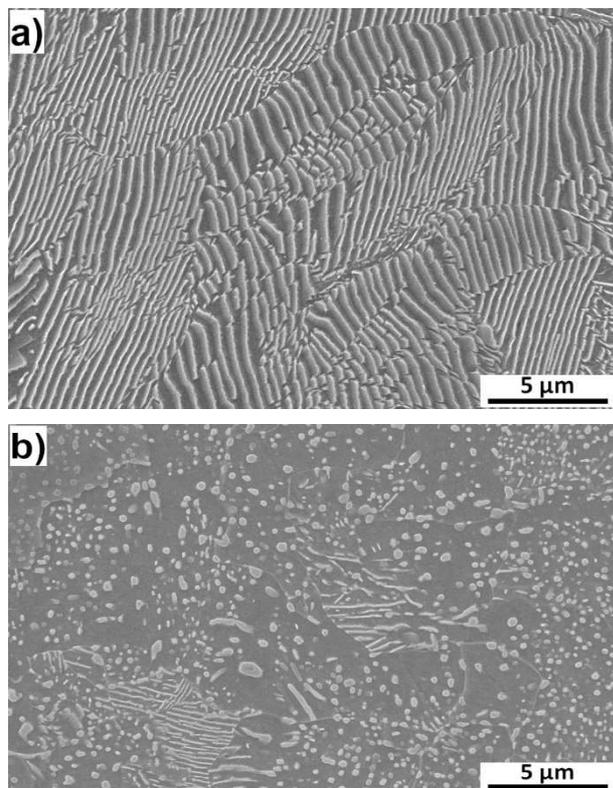
Fig. 1 *Initial microstructures - as normalized microstructure with lamellar pearlite in ferrite (a) and predominantly globular carbides in SAT-treated sample*
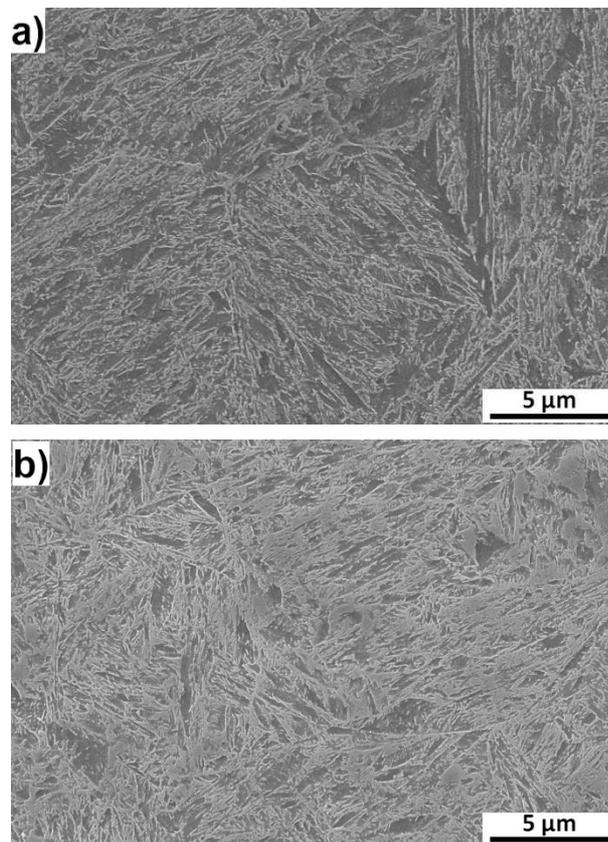
The microstructure of the as-normalized sample consisted of pearlite (lamellar cementite in ferrite). While the microstructure after ASR treatment was created by a ferrite matrix and globular particles of cementite with a diameter up to 0.5 µm. Both microstructures were compared in Fig. 1. Hardness of the as-normalised sample was determined 290 HV10 compared to the hardness of 224 HV10 after ASR.

ASR treatment was developed as a replacement for conventional soft annealing which takes several hours of duration, while the processing time of ASR is several minutes. The size and shape of carbides influence the austenitization process – finer carbides are dissoluted faster – and also mechanical properties are better for the steel with finer microstructure. The effect of ASR on properties was investigated in various steels in previous works [16–18].

After quenching from 870 °C (20 min) and tempering at 400 °C (120 min), the microstructures seemed to be similar composed of tempered martensite, transition carbides (η-Fe_2C and ε-$Fe_{2.4}C$) and cementite (Fig. 2). No significant difference in microstructures was observed. Results of the tensile test of both samples in quenched and tempered state are summarized in Tab. 2. Values of elongation, tensile strength and yield strength were slightly higher in the ASR sample. The highest difference was found in the increase in reduction of area from 16% to 22% after the treatment including ASR.


Fig. 2 *Microstructures after tempering at 400 °C - a) as-normalized initial microstructure and b) initial microstructure after ASR*

Tab. 2 *Tensile test results of as-normalized and ASR samples after tempering at 400 °C*

Sample	$R_{p0,02}$ (MPa)	R_m (MPa)	A (%)	Z (%)
QT	1667 ± 15	1867 ± 7	9 ± 1	16 ± 1
ASR+QT	1694 ± 20	1875 ± 15	10 ± 1	22 ± 1

3.2 Influence of thermomechanical treatment

Microstrutures of conventionally quenched and tempered and thermomechanical treated and tempered samples were found to be similar in SEM observation. Usual martensitic microstructures were observed composed of lath, blocks and packets, some retained austenite islands and transition carbides within martensite (Fig. 3). Defomed grains or non-recrystallized microstructure were not observed, because the thermomechanical treatment was conducted above the temperature of 800 °C [19].

TMT provided an improvement in the mechanical properties of the samples compared to quenching and tempering. Mainly, the increase in yield strength (about 130 MPa) and reduction of area (about 20%) were found. The results of tensile tests are listed in Tab. 3. In previous studies [19, 20], devoted to the effect of thermomechanical treatment on mechanical properties, the following results were obtained. A deformation prior quenching improved significantly both strength and ductility. More detailed microstructure observation was carried out and

influence on martensitic packets, blocks and laths was also described. Furthermore, the prior austenite grain boundaries (PAGB) were occupied with fine and spherical carbides in TMT samples compared to a thin carbide film in conventionally quenched and tempered samples.
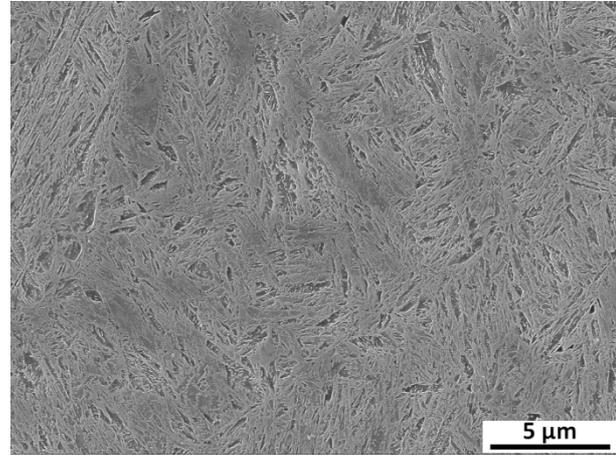
***Fig. 3*** *Microstructure of the TMT sample tempered at 250 °C*

Tab. 3 Tensile test results of conventially QT and TMT processed samples tempered at 250 °C

Sample	$R_{p0,02}$ (MPa)	R_m (MPa)	A (%)	Z (%)
QT	1893 ± 12	2278 ± 19	6 ± 2	25 ± 3
TMT	2024 ± 18	2277 ± 14	9 ± 1	45 ± 2

3.3 Influence of SAT processing

SAT processing was applied after hardening and influenced the final properties and microstructure distinct from the previous ASR treatment. The microstructures (Fig. 4) of conventional QT (tempering temperature of 300 °C) and SAT (first tempering temperature of 250 °C and second one of 300 °C) samples consisted of tempered lath martensite with transition carbides (ε- or η-carbides) and some content of retained austenite (RA). The RA contents of 5 vol.% in the SAT sample and 10 vol.% in the QT sample were determined using the Rietveld method.
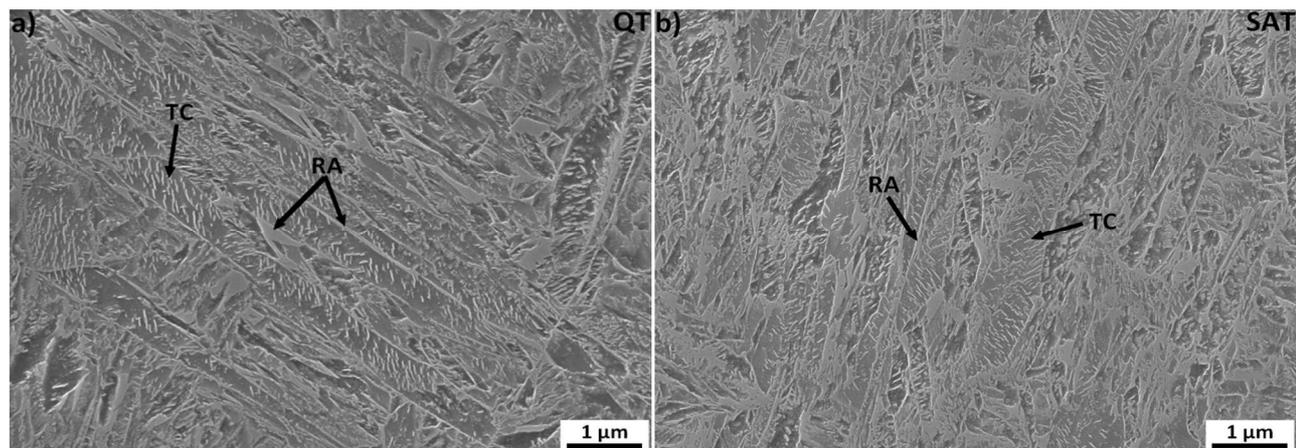

Fig. 4 *SEM-microstructure of QT (a) and SAT (b) samples with marked transition carbides (TC) inside martensite laths and retained austenite (RA)*

Furter differences in microstructures were found using EBSD analysis. The microstructure of the SAT-ed samples looked finer in the EBSD orientation maps (Fig. 5). The effective grain size represented by diameter reached values of 0.30 μm for the SAT sample

and 0.35 μm for the QT sample. However, only grain boundaries with misorientations above 15° were included in grain size estimation as in previous work [14]. While both samples varied significantly in the amount of the low-angle grain boundaries (LAGB)

with misorientation between 5° - 15°. A typical misorientation angle distribution with a peak below 10° and in the range of 54° - 60° was found for both samples, see the misorientation angle distribution in Fig. 4. The misorientation angles below 10° correspond to lath boundaries and the misorientation angles between 54–60°are characteristic of certain orientation relationships between austenite and martensite, such as Nishiyama–Wassermann and Kurdjumov–Sachs [14, 21]. The SAT sample contained a much higher amount of grain boundaries with misorientation below 10° than the QT sample, probably as a result of deformation between the first and second tempering. EBSD maps of both QT and SAT samples were collected and evaluated under the

same conditions and the total length of LAGB and HAGB provided an estimation of the number of individual types of grain boundaries. The total lengths of HAGB were 7.3 mm in the QT and 7.9 mm in the SAT sample, while the total length of LAGB in QT was significantly lower in the QT sample (0.9 mm) than in the SAT sample (2.5 mm). It seems that LAGB also contributed to higher mechanical properties of the SAT sample similar to in [22], where, moreover, the increase in mechanical properties was not attributed to higher dislocation density according to XRD results but only to grain boundary strengthening, including small-angle boundaries. Other studies also reported that also LABG influenced mechanical properties [23, 24].
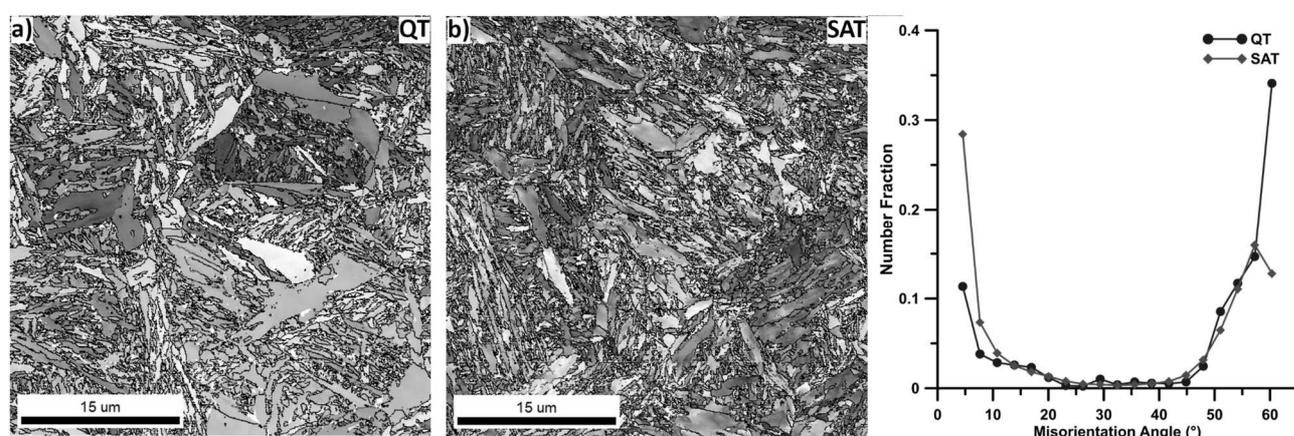
Fig. 4 *The EBSD maps of QT (a) and SAT (b) samples are colored based on orientation, with high angle boundaries (misorientation angle >15°) represented by black lines and low angle boundaries (misorientation angle >5° and <15°) are depicted as red lines. The misorienation angle distributions are shown in c)*

Representative of tensile test for SAT and QT samples are shown in Tab. 4. The yield and tensile strength reached values of 2709 MPa and 2717 MPa in the SAT sample and at the same time were higher in the SAT sample than in the QT sample about approx. 800 MPa and 500 MPa respectively. On the other side, the elongation and reduction of area were nearly two times higher in the QT sample (A = 8 %, Z = 34 %) than in the SAT sample (A = 5 %, Z = 20 %). The hardness of 682 ± 4 HV10 was

determined for the SAT treatment compared to 645 ± 2 HV10 in QT steel. Full Width at Half Maximum (FWHM) values are related to the concentration of crystal defects. FWHM results (Tab. 5) of the $(110)\alpha$ and $(200)\alpha$ showed an increase in the concentration of crystal defects in the sample after SAT. Higher values of hardness and strength in the SAT sample are in good agreement with the results of RA content, effective grain size and FWHM.

Tab. 4 *Tensile test results of conventially QT and SAT processed samples tempered at 300 °C*

Sample	$R_{p0,02}$ (MPa)	R_m (MPa)	A (%)	Z (%)
QT	1915 ± 15	2240 ± 9	8 ± 1	34 ± 4
SAT	2709 ± 8	2717 ± 7	4 ± 1	20 ± 1

Tab. 5 *Full-width at half-maximum (FWHM) of XRD peaks of (110) and (200)*

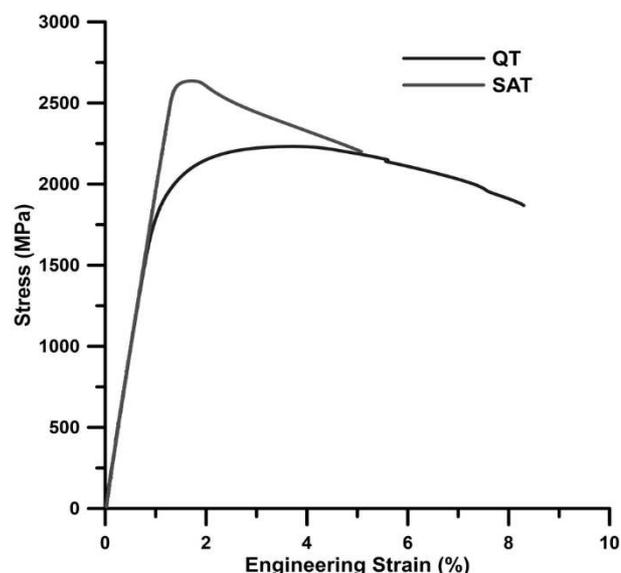| Sample	$(110)\alpha$ (mrad)	$(200)\alpha$ (mrad)
QT	8.6	17.3
SAT	9.2	18.3

Fig. 5 *Tensile engineering stress - strain digrams for QT and SAT samples tempered at 300 °C*

4 Conclusions

This study is focused on the improvement of mechanical properties of medium carbon spring steel 54SiCr6. Three technological steps were investigated.

Firstly, the influence of initial microstructure was studied and the beneficial effect of fine microstructure and carbide particles on mechanical properties after quenching and tempering was found. Mainly, the increase in the reduction of area was significant. The ASR treatment is characterized by a significant reduction in heat treatment time compared to traditional soft annealing and ensures the formation of a ferrite matrix and globular particles of cementite with a diameter of up to 0.5 µm.

Secondly, the influence of thermomechanical treatment was determined. The deformation before quenching refine the martensitic structure and the carbide thin film along PAGB was fragmented into fine and spherical carbides. The changes in microstructure caused an increase in both strength and ductility. Otherwise, a thin film of cementite may form along PAGBs and martensitic needles during tempering, causing a decrease in toughness referred to as tempered martensite embrittlement.

Finally, the modified tempering process called SAT was studied. The SAT treatment caused a decrease in effective grain size and retained austenite content. At the same time, the crystal defects concentration increased. These changes in microstructure led to an increase in hardness, tensile (increase of 800 MPa) and yield strength (increase of 500 MPa), but plastic such as elongation and reduction of area decreased. The increase in strength was attributed to grain boundary and dislocation strengthening mechanisms. The combination of these various treatments can provide steel with superior mechanical properties.

References

[1] ISO 8458-1:2002. Steel wire for mechanical springs - Part 1: General requirements; International Organization for Standardization: Geneva, Switzerland, 2002.

[2] JENÍČEK, Š., OPATOVÁ, K., HAJŠMAN, J., VOREL, I. (2022). Evolution of Mechanical Properties and Microstructure in Q&P Processed Unconventional Medium-Carbon Silicon Steel and Comparison between Q&P Processing, Quenching and Tempering, and Austemperingfor. In: *Manufacturing Technology*, Vol. 22, No. 2), pp. 146–155. ISSN 12132489.

[3] JANDA, T., JIRKOVÁ, H., JENÍČEK, Š., KUČEROVÁ, L. (2019). Influence of Cooling Rate on Microstructure and Mechanical Properties of 42SiCr Steel after Q&P Process. In: *Manufacturing Technology*, Vol. 19, No. 4, pp. 583–588. ISSN 12132489.

[4] JENÍČEK, Š., PEKOVIĆ, M., OPATOVÁ, K., VOREL, I. (2021). Relationship between mechanical properties in 42SiCr and 42SiMn medium-carbon steels and austempering temperatures. In: *Manufacturing Technology*, Vol. 21, No. 1, pp. 71–75. ISSN 12132489.

[5] HAFEEZ, M.A. (2019). Effect of microstructural transformation during tempering on mechanical properties of quenched and tempered 38CrSi steel. In: *Materials Research Express*, Vol. 6, No. 8, pp. 086552. ISSN 2053-1591.

[6] PRIMIG, S., LEITNER, H. (2011). Separation of overlapping retained austenite decomposition and cementite precipitation reactions during tempering of martensitic steel by means of thermal analysis. In: *Thermochimica Acta*, Vol. 526, No. 1–2, pp. 111–117. ISSN 00406031.

[7] SPEICH, G.R., LESLIE, W.C. (1972). Tempering of steel. In: *Metallurgical Transactions*, Vol. 3, No. 5, pp. 1043–1054. ISSN 0360-2133.

[8] NAM, W.J., CHOI, H.C. (1999). Effect of Si on mechanical properties of low alloy steels. In: *Materials Science and Technology*, Vol. 15, No. 5, pp. 527–530. ISSN 0267-0836.

[9] KWON, H., KIM, C.H. (1983). Tempered martensite embrittlement in Fe-Mo-C and

Fe-W-C steel. In: *Metallurgical Transactions A*, Vol. 14, No. 7, pp. 1389–1394. ISSN 0360-2133.

[10] TAVARES, S.S.M., DA CUNHA, R.P.C., BARBOSA, C., ANDIA, J.L.M. (2019). Temper embrittlement of 9%Ni low carbon steel. In: *Engineering Failure Analysis*, Vol. 96, pp. 538–542. ISSN 13506307.

[11] ZIA-EBRAHIMI, F., KRAUSS, G. (1984). Mechanisms of tempered martensite embrittlement in medium-carbon steels. In: *Acta Metallurgica*, Vol. 32, No. 10, pp. 1767–1778. ISSN 00016160.

[12] SALVETR, P., GOKHMAN, A., DONIK, Č., NOVÝ, Z., KOTOUS, J., GODEC, M. (2023). EVOLUTION OF MICROSTRUCTURE AND EMBRITTLEMENT DURING THE TEMPERING PROCESS IN SiCrCu MEDIUM-CARBON STEELS. In: *Materiali in Tehnologije*, Vol. 57, No. 3, pp. 233–240. ISSN 1580-3414.

[13] SALVETR, P., GOKHMAN, A., SVOBODA, M., DONIK, Č., PODSTRANSKÁ, I., KOTOUS, J., NOVÝ, Z. (2023). Effect of Cu Alloying on Mechanical Properties of Medium-C Steel after Long-Time Tempering at 500 °C. In: *Materials*, Vol. 16, No. 6, pp. 2390. ISSN 1996-1944.

[14] KIM, B., BOUCARD, E., SOURMAIL, T., SAN MARTÍN, D., GEY, N., RIVERA-DÍAZ-DEL-CASTILLO, P.E.J. (2014). The influence of silicon in tempered martensite: Understanding the microstructure–properties relationship in 0.5–0.6wt.% C steels. In: *Acta Materialia*, Vol. 68, pp. 169–178. ISSN 13596454.

[15] HALFA, H. (2014). Recent Trends in Producing Ultrafine Grained Steels. In: *Journal of Minerals and Materials Characterization and Engineering*, Vol. 02, No. 05, pp. 428–469. ISSN 2327-4077.

[16] DLOUHY, J., HAUSEROVA, D., NOVY, Z. (2016). Influence of the carbide-particle spheroidisation process on the microstructure after the quenching and annealing of 100CrMnSi6-4 bearing steel. In: *Materiali in tehnologije*, Vol. 50, No. 1, pp. 159–162. ISSN 15802949.

[17] HAUSEROVA, D., DLOUHY, J., KOTOUS, J. (2017). Structure Refinement of Spring Steel 51Crv4 after Accelerated Spheroidisation. In: *Archives of Metallurgy and Materials*, Vol. 62, No. 3, pp. 1473–1477. ISSN 2300-1909.

[18] KOTOUS, J., DLOUHY, J., NACHAZELOVA, D., HRADIL, D. (2018). Accelerated Carbide Spheroidisation and Refinement in Spring Steel 54SiCr6. In: *IOP Conference Series: Materials Science and Engineering*, Vol. 461, pp. 012044. ISSN 1757-899X.

[19] BARANI, A.A., PONGE, D., Optimized Thermomechanical Treatment for Strong and Ductile Martensitic Steels. In: *Materials Science Forum*, 2007, p. 4526–4531, ISBN 0878494286.

[20] ARDEHALI BARANI, A., PONGE, D., RAABE, D. (2006). Refinement of grain boundary carbides in a Si–Cr spring steel by thermomechanical treatment. In: *Materials Science and Engineering: A*, Vol. 426, No. 1–2, pp. 194–201. ISSN 09215093.

[21] MORITO, S., TANAKA, H., KONISHI, R., FURUHARA, T., MAKI, T. (2003). The morphology and crystallography of lath martensite in Fe-C alloys. In: *Acta Materialia*, Vol. 51, No. 6, pp. 1789–1799. ISSN 13596454.

[22] SALVETR, P., ŠKOLÁKOVÁ, A., KOTOUS, J., DRAHOKOUPIL, J., MELZER, D., JANSA, Z., DONIK, Č., GOKHMAN, A., NOVÝ, Z. (2023). Effect of Double-Step and Strain-Assisted Tempering on Properties of Medium-Carbon Steel. In: *Materials*, Vol. 16, No. 5, pp. 2121. ISSN 1996-1944.

[23] DU, C., HOEFNAGELS, J.P.M., VAES, R., GEERS, M.G.D. (2016). Block and sub-block boundary strengthening in lath martensite. In: *Scripta Materialia*, Vol. 116, pp. 117–121. ISSN 13596462.

[24] SUN, C., FU, P., LIU, H., LIU, H., DU, N., CAO, Y. (2020). The Effect of Lath Martensite Microstructures on the Strength of Medium-Carbon Low-Alloy Steel. In: *Crystals*, Vol. 10, No. 3, pp. 232. ISSN 2073-4352.